Reorienting Interfacial Water via Nanostructure Tip Effect to Accelerate Oxygen Reduction Kinetics

Pengbo Wang,[a,b] Youze Zeng,[a,b] Xukai Wang,[a,b] Xiaohu Liu,[a,b], Meiling Xiao,[*a,b,c] Jianbing Zhu[*a,b,c]

a School of Applied Chemistry and Engineering, University of Science and Technology of China, Hefei, Anhui, 230026, P. R. China

b Hydrogen Energy Industry Institute of Jilin Province, Changchun Institute of Applied Chemistry, Chinese Academy of Sciences, Changchun, 130022, China.

c CIAC - HKUST Joint Laboratory for Hydrogen Energy, Changchun, Jilin, 130022, P. R. China

E-mail: zjb@ciac.ac.cn (Jianbing. Zhu); mlxiao@ciac.ac.cn (Meiling. Xiao).

Supporting Information

Experimental section

Reagents and materials

Zinc acetate anhydrous (99%), 2,5-dihydroxyterephthalic acid (98%, HPLC), and urea (99%) were purchased from Aladdin. Methanol (AR) was obtained from Xilong Scientific Co., Ltd., Deuterium oxide (99.9%) was purchased from Innochem.

Synthesis of Zn-MOF-74

Zn-MOF-74: A solution of 2,5-dihydroxyterephthalic acid (0.3 mmol) in methanol (50 mL) was prepared under ultrasonication (denoted as Solution A). Separately, anhydrous zinc acetate (1.0 mmol) was dissolved in methanol (100 mL) via ultrasonication (denoted as Solution B). Subsequently, Solution A was added dropwise into Solution B under continuous ultrasonication. The mixture was further sonicated for 30 minutes. The resulting precipitate was collected and washed, yielding the as-synthesized Zn-MOF-74 particles.

Sea-Urchin-Like Zn-MOF-74 (Zn-MOF-74-S): The obtained Zn-MOF-74 particles were uniformly dispersed in deionized water (15 mL) and mixed with urea (100 mg). The suspension was transferred into a 50 mL Teflon-lined autoclave and subjected to a solvothermal treatment at 180 ℃ for 24 h. The dark-brown product was collected by filtration, thoroughly washed with deionized water, and dried overnight at 60 ℃.

Synthesis of N-doped Carbon (NC)

Sea-Urchin-Like NC (NC-S): The obtained Zn-MOF-74-S was placed in a tube furnace with urea positioned upstream as a solid nitrogen source. Pyrolysis was conducted under Ar atmosphere with a heating rate of 5 ℃ min^{-1} to 910 ℃, followed by 2 h hold at the target temperature. The furnace was then allowed to cool naturally to room temperature.

Conventional NC (NC): For comparison, conventional NC was prepared following an identical pyrolysis procedure, using the Zn-MOF-74 particles as the precursor instead.

Larger special surface area NC(NC-L): 100 mg of synthesized Zn-MOF-74 was mixed uniformly with 10 wt.% NH4HCO3 and then pyrolyzed. The remaining parameters were exactly the same as those for the synthesis of NC/NC-S.

Synthesis of Fe-N-C-S

FeNC-S: 100 mg of the NC-S was first dispersed in 50 mL of methanol via ultrasonication. Subsequently, 10 mg of $FeCl_2 \cdot 4H_2O$ was added to the suspension. The mixture was stirred at room temperature for 24 h to ensure thorough adsorption and dispersion of the iron precursor. The solid product was then isolated via vacuum filtration, washed with methanol, dried, and then subjected to a second pyrolysis step. This thermal treatment was performed under an Ar atmosphere at 900 ℃ (heating rate: 10 ℃ min^{-1}) for 2 h, yielding the final catalyst denoted as FeNC-S.

FeNC: As a control sample, the FeNC was synthesized using the exact same iron loading and pyrolysis protocol, but with NC as the supporting material.

FeNC-L: The synthesis method of FeNC-L was exactly the same as that of FeNC-S, except that NC was replaced with NC-L

Physical Characterization

X-ray diffraction (XRD) patterns were recorded on a Bruker D8 ADVANCE diffractometer using Cu Kα radiation source (λ=1.54 Å). Scanning electron microscopy (SEM) measurements were performed with an XL30 ESEM FEG field emission scanning electron microscope. Specific surface areas and pore size distributions were obtained from nitrogen sorption isotherms at 77 K (Micromeritics ASAP 2020). X-ray photoelectron spectroscopy (XPS) measurements were carried out on Thermo Scientific K-Alpha.

Electrochemical Measurements

The electrocatalytic ORR properties, including activity and selectivity, were characterized using a CHI750E electrochemical workstation at room temperature. Measurements were performed in a three-electrode setup featuring a rotating disk electrode (RDE) or a rotating ring-disk electrode (RRDE) as the working electrode, a graphite rod as the counter electrode, and a saturated calomel electrode (SCE) equipped

with a salt bridge served as the reference electrode. All the potentials were calibrated to the reversible hydrogen electrode (RHE) according to the Nernst equation. (E_{RHE} = E_{SCE} + 0.059pH + 0.244 V).

A uniformly dispersed catalyst ink was obtained by sonicating for at least 30 minutes a mixture containing 5 mg catalyst, 450 μL ethanol, and 50 μL Nafion (5 wt%). A certain volume of the ink was then drop-cast onto the working electrode using a micropipette. The electrode was rotated until the ink dried naturally under room temperature, resulting in a uniformly coated working electrode. The catalyst loading was controlled at 0.6 mg_{cat} cm^{-2}, while the commercial Pt/C catalyst was loaded at 0.02 mg_{Pt} cm^{-2}.

The linear sweep voltammetry (LSV) measurements were performed in O_2-saturated 0.1 M KOH solution over a potential range of 0 V to 1.1 V at a scan rate of 5 mV s^{-1}, with rotation speeds varying from 900 rpm to 2025 rpm. In rotating ring-disk electrode (RRDE) tests, the ring potential was set to 1.3 V. All current densities were normalized to the geometric area of the RDE or RRDE. Cyclic voltammetry (CV) scans were conducted at different scan rates (5, 10, 15, 20, 25 mV s^{-1}) within a non-Faradaic potential window to calculate the double-layer capacitance (C_{dl}) of the prepared cathode materials. Accelerated durability tests (ADTs) were carried out in an O_2-saturated 0.1 M KOH solution by cycling the potential between 0.6 V and 1.0 V at a scan rate of 200 mV s^{-1}.

The kinetic current density (j_k) is calculated to the equation:

$$\frac{1}{j_m} = \frac{1}{j_L} + \frac{1}{j_k} \quad (1)$$

where j_m indicates the measured total current density and j_L is the diffusion-limiting current density.

The electron transfer number (n) per oxygen molecule was calculated from the Koutecky-Levich (K-L) equations:

$$\frac{1}{j} = \frac{1}{J_k} + \frac{1}{B}\omega^{-1/2} \quad (2)$$

$$B = 0.2nF(Do_2)^{2/3}\nu^{(-1/6)}C_{(o_2)} \quad (3)$$

where ω is the angular velocity of the disk (rpm), n is the electron transfer number for ORR, F is Faraday constant (96485 C mol^{-1}), D_{O2} is the diffusion coefficient of O_2 in 0.1 M KOH (1.9×10^{-5} cm^2 s^{-1}), ν is the kinematic viscosity (0.01 cm^2 s^{-1}), C_{O2} is the bulk concentration of O_2 in the solution (1.2×10^{-6} mol cm^{-3}).

With a collection efficiency (N) of 0.37, the electron transfer number(n) and the HO_2^- yield were calculated based on the following equations derived from RRDE measurements.

$$HO_2^- = 200 \times \frac{I_R/N}{I_D + I_R/N} \quad (4)$$

$$n = \frac{4I_D}{I_D + I_R/N} \quad (5)$$

Where I_R is the ring current, and I_D is the disk current.

Determination of site density (SD) and turnover frequency (TOF) by nitrite stripping

An electrode with a catalyst loading of 0.27 mg cm^{-2} was drop-coated in a 0.5 M sodium acetate buffer (pH 5.2). After cleaning the catalyst surface following the procedure described in the literature[1], a cyclic voltammogram (CV) was recorded in an N_2-saturated 0.5 M sodium acetate solution over the potential range of -0.3 to 0.4 V (vs. RHE) to obtain the background curve prior to nitrite poisoning. The electrode was then immersed in a 0.125 M $NaNO_2$ solution for 5 minutes, followed by sequential washing with deionized water, sodium acetate solution, and deionized water to obtain a nitrite-ion-poisoned electrode. Subsequently, a CV for nitrite reduction was performed in an N_2-saturated 0.5 M sodium acetate solution from -0.3 to 0.4 V (vs. RHE). Finally, a second CV scan was conducted in the same solution and potential range to obtain the recovery curve. The site density was calculated using the following equation:

$$SD[site \cdot g^{-1}] = \frac{Q_{Str} \times N_A}{n_{Str} \times F} \quad (6)$$

Where Q_{str} is the nitrite reductive stripping charge determined from the stripping peak, n_{str} is the number of electrons associated with the reduction of one adsorbed nitrosyl per site and its value is 5, N_A is Avogadro constant (6.022×10^{23} mol^{-1}) and F is Faraday constant (96485 C mol^{-1}).

The turnover frequency (TOF) was calculated by the following equation:

$$TOF\left[e^{-1}s^{-1}site^{-1}\right] = \frac{jk \times N_A}{SD \times F} \tag{7}$$

Where j_k is the kinetic current density at 0.90V vs. RHE.

Isotopic labeling experiments

To study the kinetic isotope effect (KIE), 0.1M KOH solutions were prepared with Milli-Q water (18.25 MΩ cm^{-1}) and D_2O, respectively. LSV tests were conducted in these solutions, and the electrochemical experiments were carried out according to the above experimental conditions. The electrochemical experiments were conducted using the same procedure described above.

The KIE is the ratio of constants (k_f^H / k_f^D), which can be calculated at a selected potential.[2]

$$KIE = \frac{k_f^H}{k_f^D} = \frac{j_k^H n^D F C_{O_2}^{*,D}}{j_k^D n^H F C_{O_2}^{*,H}} \tag{8}$$

where

$$\frac{C_{O_2}^{*,D}}{C_{O_2}^{*,H}} = 1.101 \quad \text{(298K)} \tag{9}$$

due to the difference in the solubility of O_2 in D_2O and H_2O. By assuming that the electron count (number of electrons transferred) $n^D = n^H$, the KIE can then be calculated as:

$$KIE = \frac{k_f^H}{k_f^D} = \frac{j_k^H n^D F C_{O_2}^{*,D}}{j_k^D n^H F C_{O_2}^{*,H}} = 1.101 \frac{j_k^H}{j_k^D} \quad (10)$$

Fuel cell MEA tests

The performance of the anion exchange membrane fuel cell (AEMFC) with FeNC-S cathode was evaluated using the DC 980 PEM Fuel Cell Testing System (DC-Energies). The synthesized catalyst was dispersed in an isopropanol/water (1:1) solution containing PiperIon ionomer (PiperION-A5-HCO3-EtOH). The ink was ultrasonicated for 2 h and subsequently uniformly sprayed onto the gas diffusion layer (XGL-R055). The prepared cathode had an active area of 4 cm^2 with a catalyst loading of 2.5mg cm^{-2}. The electrode and anion exchange membrane (PiperIOn A20-HCO_3, 20μm thick) were immersed in a 1M KOH solution at 60°C for 4 h to facilitate ion exchange. Afterward, the exchanged electrode and membrane were assembled into a fuel cell. The anode was fabricated using PtRu/C as the catalyst. During the membrane electrode assembly (MEA) tests, the cell and gas humidifier temperatures were maintained at 80 °C with 100% relative humidity. The backpressure of hydrogen and oxygen or air was set to 0.1MPa, with gas flow rates of 0.5 L min^{-1} for hydrogen and 1.5 L min^{-1} for oxygen/air, respectively.

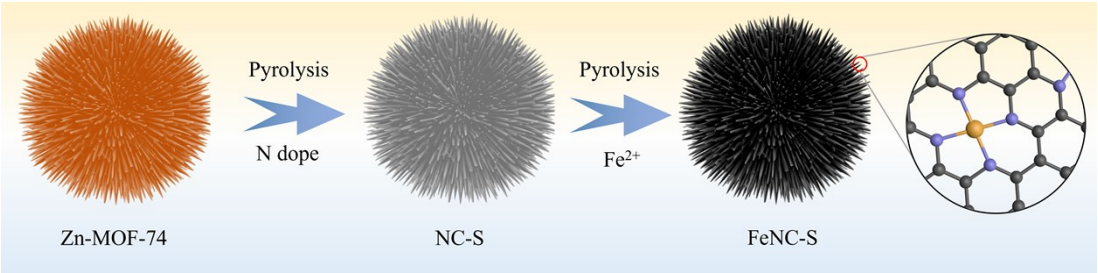

Fig. S1. Schematic illustration for the preparation process of FeNC-S.

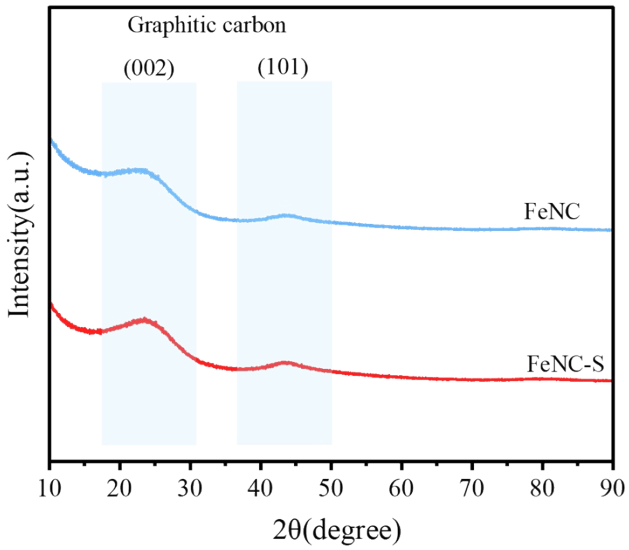

Fig. S2. XRD pattens of FeNC-S and FeNC.

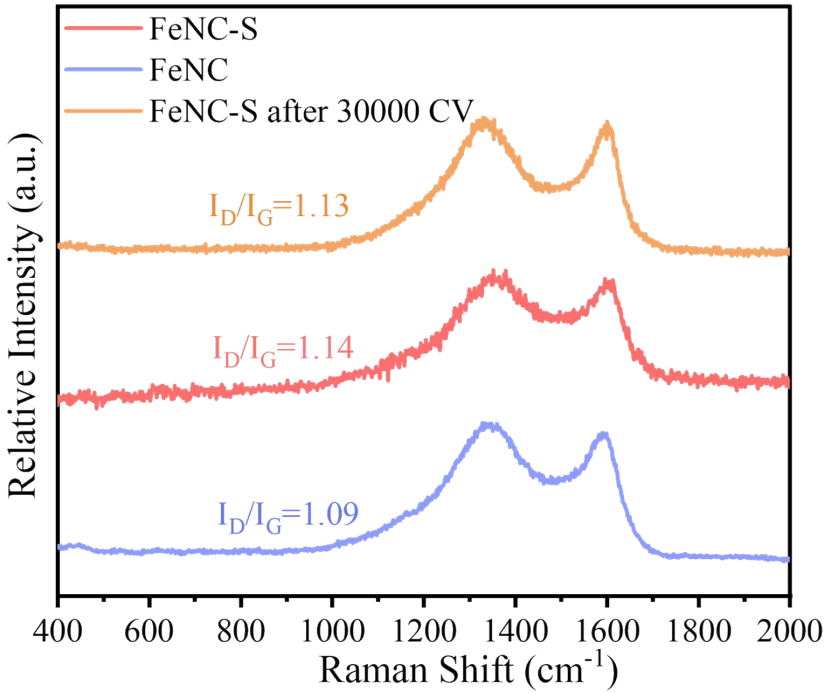

Fig. S3. Raman spectra of FeNC, FeNC-S and FeNC-S after 30,000 Cycles.

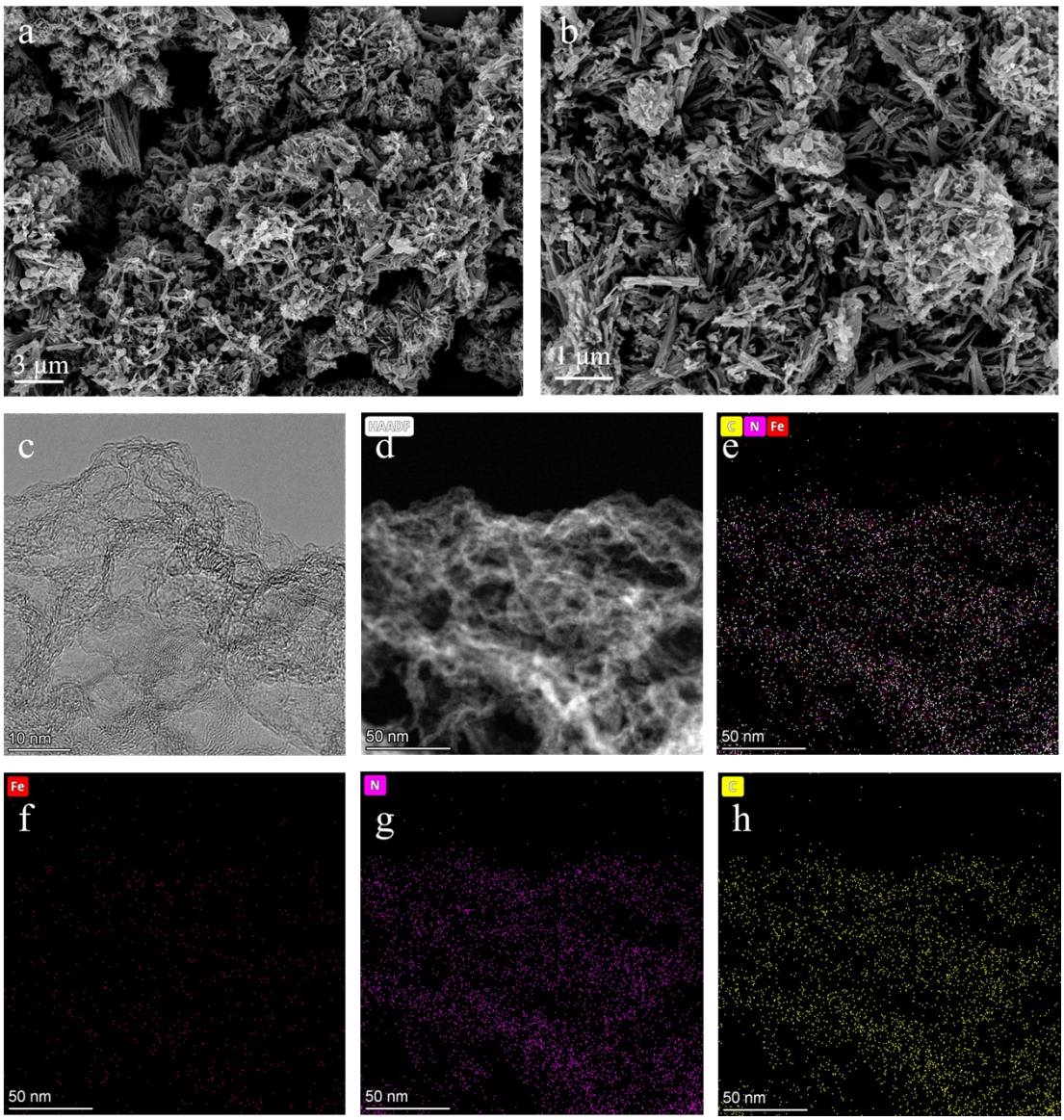

Fig. S4. Structural characterization of FeNC morphology. a) b) SEM images at different scales. c) HRTEM images. d) HAADF-STEM images. e-h) The corresponding elemental mapping images.

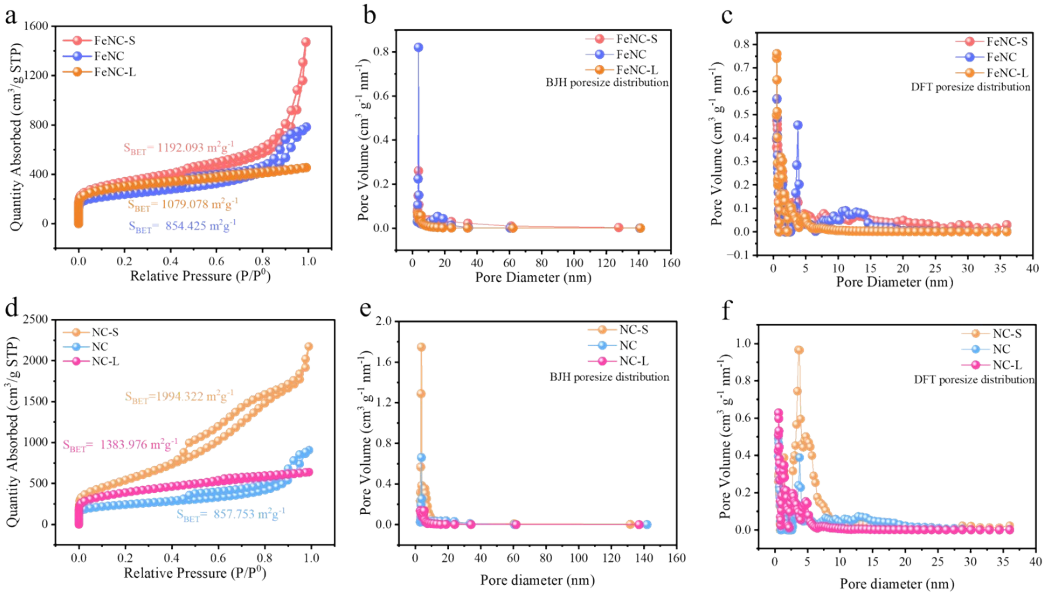

Fig. S5. The nitrogen adsorption-desorption isotherms and the corresponding pore-size distribution plots for NC, NC-S, NC-L, FeNC, FeNC-S, FeNC-L.

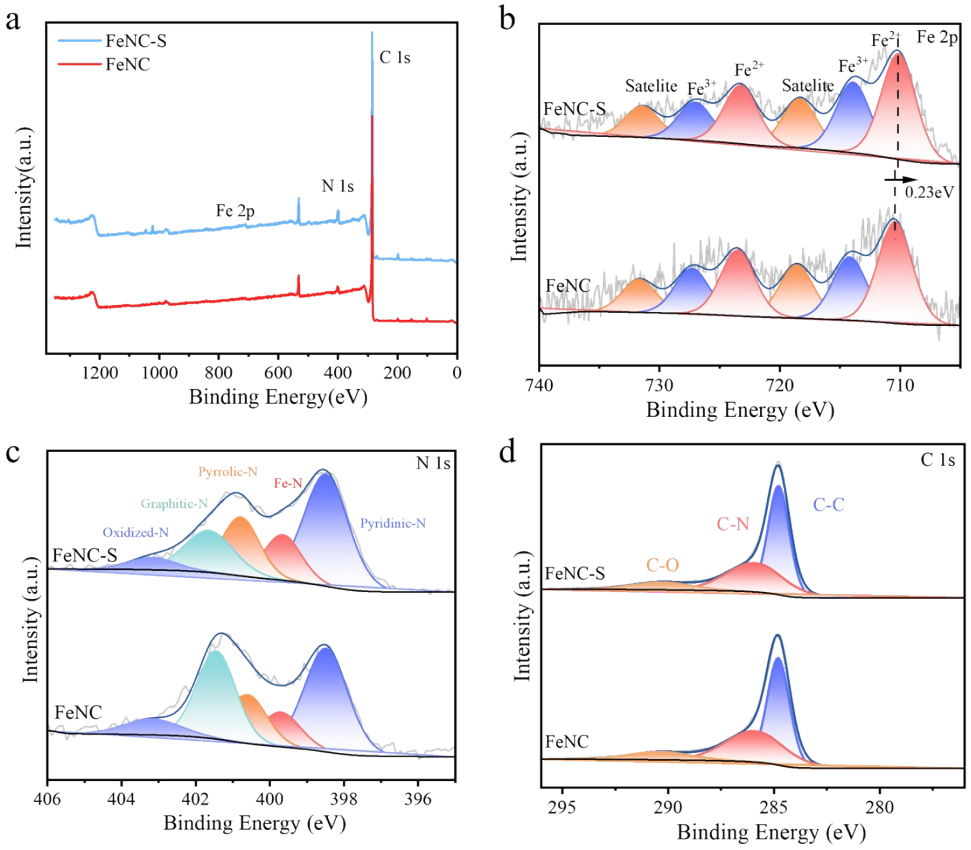

Fig. S6. a) XPS survey spectra, b) Fe 2p spectra, c) N1s spectra, d) C 1s spectra of FeNC-S and FeNC.

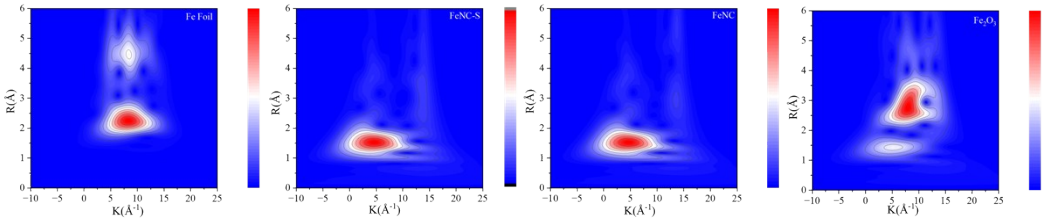

Fig. S7. The WT-EXAFS images of different catalysts.

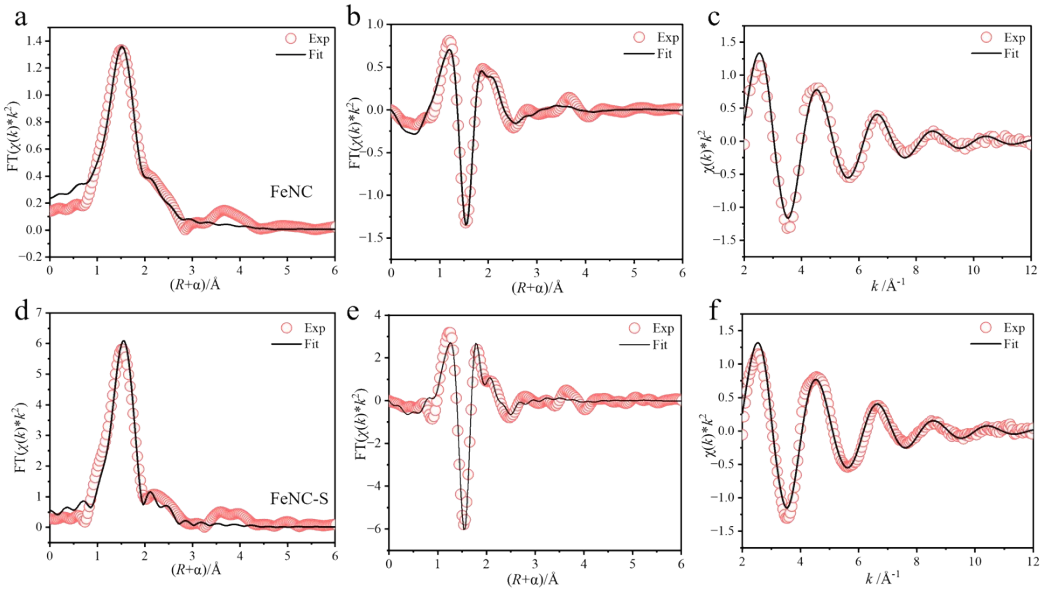

Fig. S8. Fe K-edge EXAFS and curve fit for FeNC, shown in R-space (FT magnitude (a) and imaginary component (b)). (c) Fe K-edge EXAFS and curve fit for FeNC, shown in k^2-weighted k-space. Fe K-edge EXAFS and curve fit for FeNC-S, shown in R-space (FT magnitude (d) and imaginary component (e)). (f) Fe K-edge EXAFS and curve fit for FeNC-S, shown in k^2-weighted k-space.

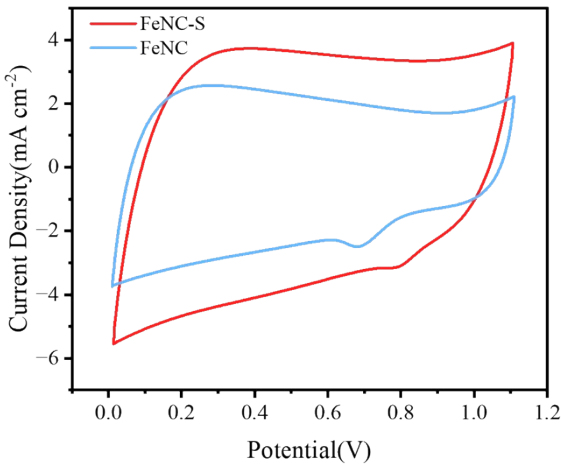

Fig. S9. CV curves of FeNC and FeNC-S.

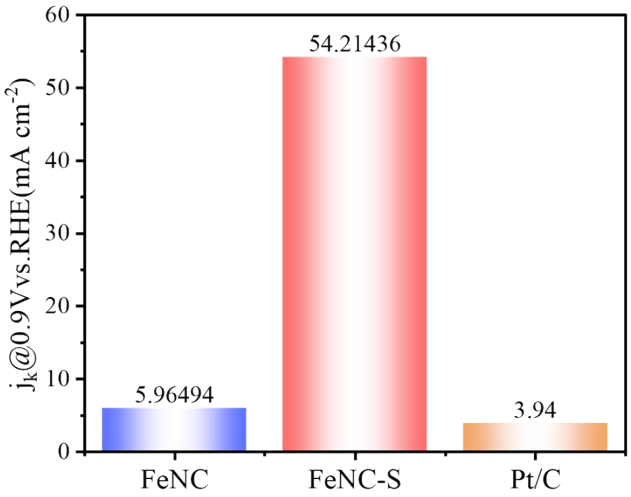

Fig. S10. The kinetic current density of FeNC-S, FeNC and Pt/C at 0.9V.

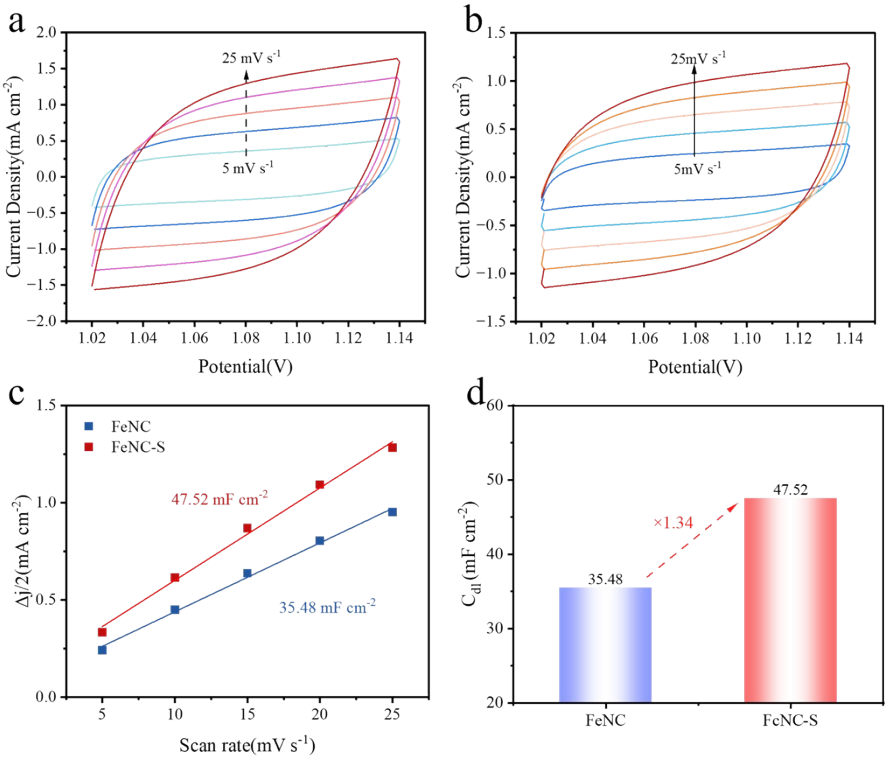

Fig. S11. CV curves at various scan rates and the corresponding C_{dl} of FeNC-S and FeNC.

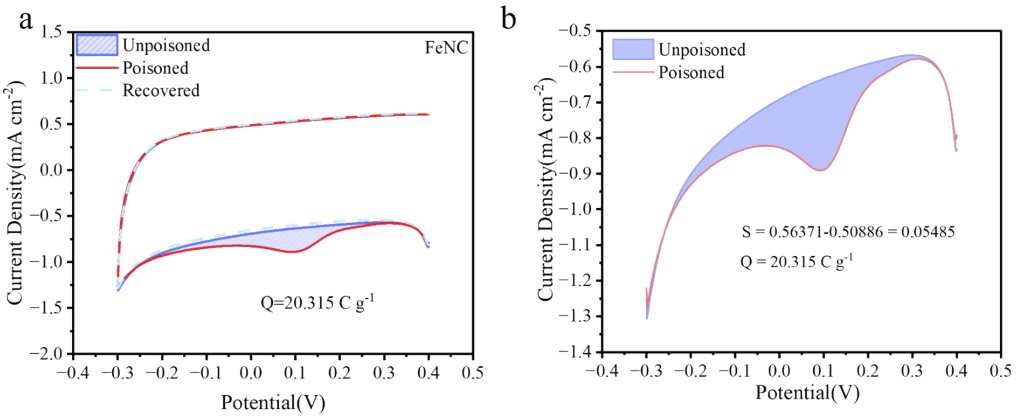

Fig. S12. a) CV curves of FeNC during the nitrite stripping experiment at the unpoisoned, poisoned, and recovered stages. b) The integration range of the nitrite stripping experiment and the calculated Q value.

Note S1: The detailed calculation process is as follows, taking FeNC as an example. The area of the shaded region in Figure d is integrated to obtain ΔS, The catalyst loading on the electrode is 0.27 mg cm^{-2}, where $Q = \int I\,dt$. The calculated ΔS is 0.05485, corresponding to Q = 20.315 C g^{-1}.

According to Equation S6 in the Supporting Information, the site density SD [site g^{-1}] is calculated as $SD = (Q \times N_A) / (n \times F)$, where Q = 20.315 C g^{-1}, $N_A = 6.022 \times 10^{23}$, n = 5, and F = 96485 C mol^{-1}. The calculated SD is 2.536×10^{19} site g^{-1}. Simultaneously, following Equation S7 in the Supporting Information, the kinetic current density j_k at 0.9 V obtained from the LSV curve for the FeNC sample is 5.965 mA cm^{-2}. The turnover frequency (TOF) is then calculated as $TOF = (j_k \times N_A) / (SD \times F)$, yielding a value of 1.468 e^{-1} $site^{-1}$ s^{-1}. The corresponding values for FeNC-S were obtained using the same calculation method.

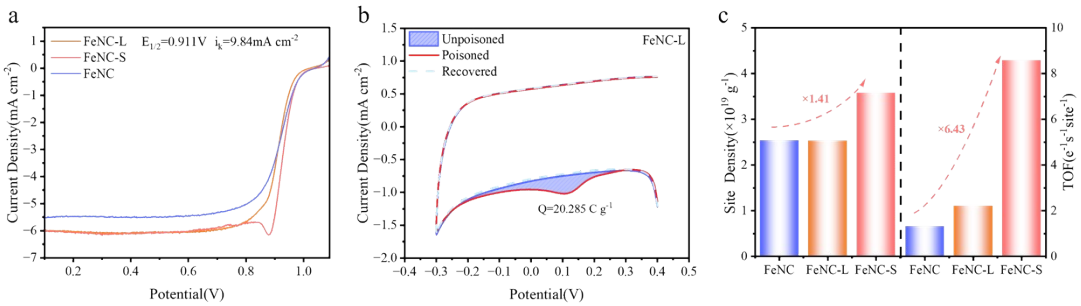

Fig. S13 a) LSV curves of FeNC-S, FeNC and FeNC-L. b) Nitrite stripping CV curves of FeNC-L. c) SD and TOF values for FeNC-S, FeNC and FeNC-L.

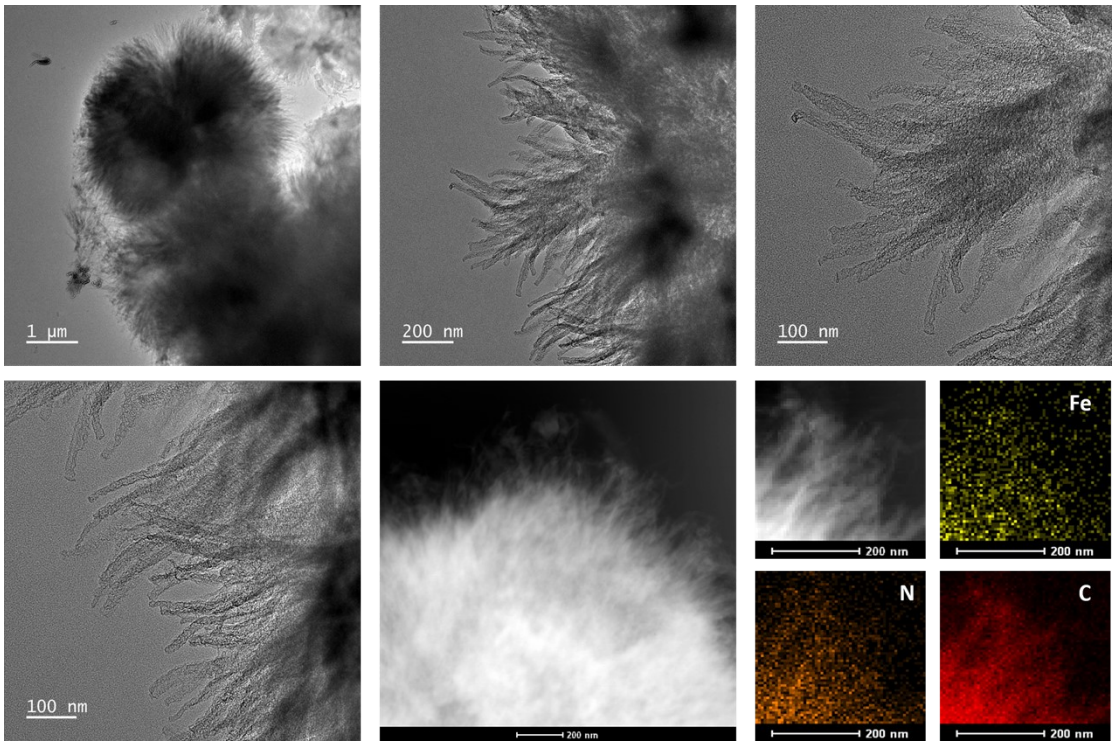

Fig. S14. TEM image and corresponding elemental mapping of FeNC-S after 30,000 CV cycles

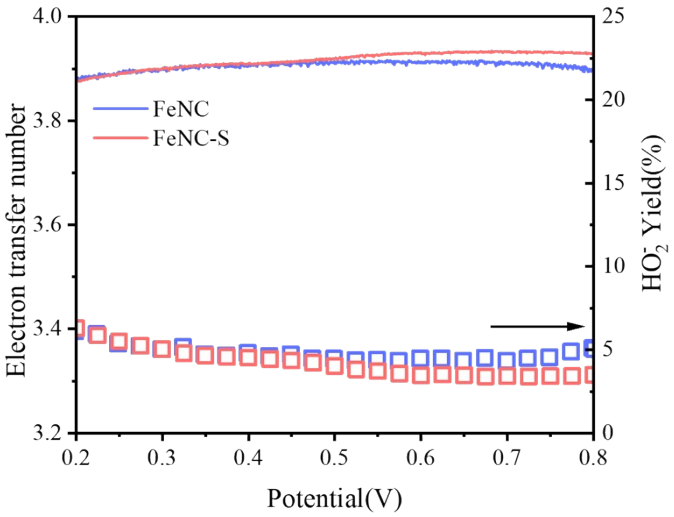

Fig. S15. the HO_2^- yield and the corresponding electron transfer number(n) of these samples

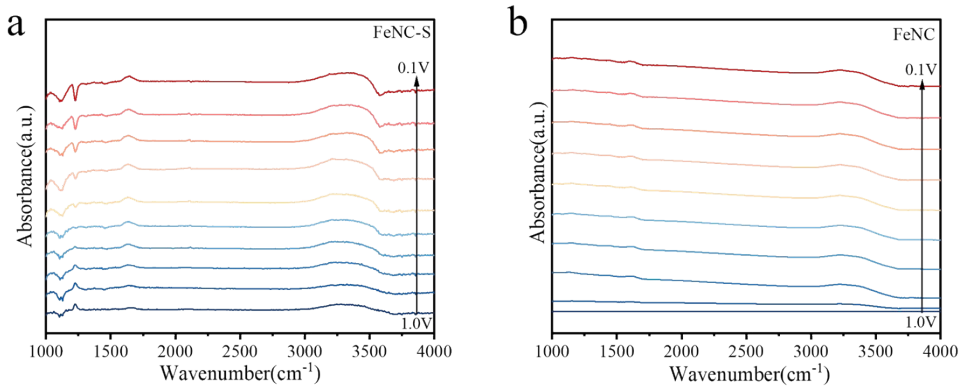

Fig. S16. In-situ ATR-IR analysis of the FeNC-S and FeNC.

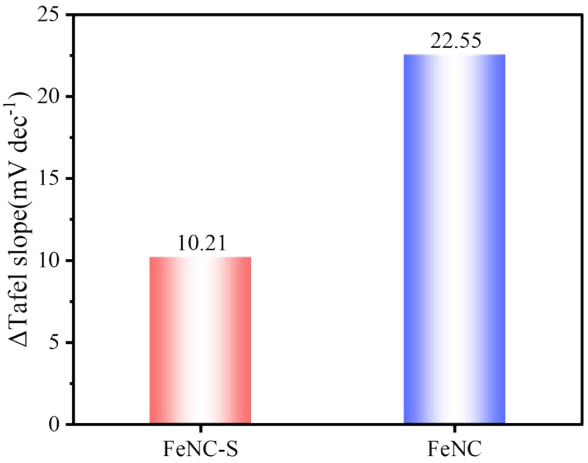

Fig. S17. Variation of Tafel slopes of FeNC and FeNC-S catalyst tested in 0.1 M KOH electrolytes prepared with H_2O and D_2O.

Table S1. BET results of carbon supports and catalysts.

	$S_{BET}(m^2 g^{-1})$	Pore Volume ($cm^3 g^{-1}$)	Pore width (nm)
NC	857.753	1.238	0.548
NC-S	1994.322	3.261	3.627
NC-L	1383.976	0.461	0.573
FeNC	854.425	1.935	0.573
FeNC-S	1192.093	1.042	2.866
FeNC-L	1079.078	0.265	0.548

Table S2. The element contents measured by XPS for different samples.

	Fe(at%)	N (at%)	C (at%)
FeNC	0.42	4.05	95.53
FeNC-S	0.57	6.07	93.35

Table S3. The proportion of different carbon types calculated from the peak area ratio in C 1s XPS spectra.

	C-C	C-N	C-O
FeNC	52.12%	37.09%	10.77%
FeNC-S	50.82%	38.90%	10.28%

Table S4. The proportion of different nitrogen types calculated from the peak area ratio in N 1s XPS spectra.

	Pyridinic-N	Fe-N	Pyrrolic-N	Graphitic-N	Oxidized-N
FeNC	37.09%	11.33%	15.63%	28.57%	7.38%
FeNC-S	43.20%	14.82%	19.04%	17.92%	5.03%

Table S5. EXAFS fitting parameters at the Fe K-edge for FeNC and FeNC-S.

	Path	CN	R(Å)	σ^2	ΔE_0(eV)	R-factor	S_0^2
FeNC	Fe-N	4	1.99122	0.00930	9.123	0.0118579	0.963
FeNC-S	Fe-N	4	1.99224	0.00917	9.262	0.0124191	0.946

CN is the coordination number; R is the interatomic distance; σ^2 is the Debye-Waller factor; ΔE_0 is the inner potential correction; R factor indicates the goodness of the fitting.

Table S6. The nitrite stripping charge of FeNC, FeNC-S, and FeNC-L samples, along with the calculated site densities (SD) and TOF values.

	Q_{str} (C g^{-1})	SD ($\times 10^{19}$)	TOF (e^{-1} s^{-1} $site^{-1}$)
FeNC	20.315	2.536	1.468
FeNC-S	28.737	3.587	9.433
FeNC-L	20.285	2.532	2.425

References:

1. D. Malko, A. Kucernak and T. Lopes, *Nat. Commun.*, 2016, **7**, 3285.
2. Y. Wang, Y. Yang, S. Jia, X. Wang, K. Lyu, Y. Peng, H. Zheng, X. Wei, H. Ren, L. Xiao, J. Wang, D. A. Muller, H. D. Abruña, B. J. Hwang, J. Lu and L. Zhuang, *Nat. Commun.*, 2019, **10**, 1506.